DEPARTMENT OF
MINERALS AND ENERGY

BUREAU OF MINERAL RESOURCES, GEOLOGY AND GEOPHYSICS

RECORD 1974/55

FAULTING ASSOCIATED WITH THE MAJOR NORTH SOLOMON SEA EARTHQUAKES OF 14 and 26 July 1971

by

I.B. EVERINGHAM

RECORD 1974/55

FAULTING ASSOCIATED WITH THE MAJOR NORTH SOLOMON SEA EARTHQUAKES OF 14 AND 26 JULY 1971

by

I.B. EVERINGHAM

CONTENTS

TABLES

ILLUSTRATIONS

SUMMARY

Major tsunamigenic earthquakes occurred on 14 July and 26 July 1971 about 100 km apart in the north Solomon Sea. The second earthquake is not considered to be an aftershock of the first: aftershock patterns and fault-plane solutions indicate that both were the result of movements along two separate parts of a major fault surface. The first earthquake caused movement along the part of the fault that extends south-southeast from southernmost New Ireland; movement caused by the second earthquake was in the part of the fault that extends west-southwest from southernmost New Ireland.

The two aftershock zones overlapped to the south-southeast of New Ireland near the epicentre of the 26 July earthquake and where its fault rupture commenced. The rupturing was probably due to the effects of the 14 July earthquake series.

Aftershock and first-motion data indicate that the area between Bougainville Island, southern New Ireland, and southeastern New Britain is being underthrusted from the south. The fault surface appears to be concave downwards, with depth and dip increasing towards the islands to the northwest, north, and northeast.

During both earthquakes, intensities of at least MM8 were experienced; their isoseismals form ellipses whose long axes coincide with the trend of the relevant aftershock zone (i.e., south-southeast for the first earthquake, west-southwest for the second). Maximum intensities apparently occurred above the aftershock region.

Evidence suggests a surface-wave magnitude of 8.0 for both earthquakes.

INTRODUCTION

Earthquakes with magnitude (M) 8 or more are rare events which have occurred on average about once per year (in the 42-year period, 1904-1945; Gutenberg & Richter, 1954). Although Papua New Guinea is situated in the seismically active region surrounding much of the Pacific Ocean, only two earthquakes (September 1906 and May 1919) with magnitude 8 or greater had been recorded there since 1900, so that it was surprising when two earthquakes of magnitude about 8 occurred in the north Solomon Sea region (Fig. 1) within a 12-day period in July 1971. Earthquake detail determined by the US Environmental Research Laboratories (ERL) are as follows:

Date	H (UT)	Lat°S	Long°E	Depth (km)	MB(ERL)	MS(ERL)
July 14	061129.1	5.47	153.88	47	6.3	7.9
July 26	012321.3	4.94	153.17	48	6.3	7.9

The earthquakes happened in a region where seismic activity is greater than elsewhere in Papua New Guinea (Brooks, 1965; Denham, 1969; Curtis, 1973a) and where the Solomon Sea Plate is being rapidly subducted, resulting in the formation of the New Britain/Bougainville Trench and island-arc structures (Denham, 1969; Johnson & Molnar, 1972; Luyendyk, MacDonald & Bryan, 1973). The main features are shown in Figure 1.

To determine the type of faulting which took place on each occasion and whether or not the second earthquake was an aftershock of the first, a study of the isoseismals, aftershock patterns, and fault-plane solutions was made. Some of the results were also used to check the ERL magnitude determinations.

ISOSEISMALS

Figures 2 and 3 show the isoseismal maps; mean isoseismal radii are listed in Table 1. A brief description of the macroseismic effects of the earthquakes is given by Everingham (in press).

Although mean isoseismal radii were roughly the same for the two earthquakes, the trend of each set of isoseismals differed. Elliptical isoseismals for intensities MM 6-8 for the first earthquake trended north-northwest, at right-angles to those for the second; thus, even though the epicentre of the second earthquake was closer to Rabaul, its intensities were fortunately lower there than they were for the first earthquake. The reason for the differences in isoseismal trends becomes clear if the aftershock patterns are considered.

AFTERSHOCKS AND THE FAULT SURFACE

In the following discussion of aftershock data, it is assumed, on the basis of Dieterich's (1972) results, that aftershocks occur at, or very close to, the fault surface of the principal earthquake.

Figure 4 shows the aftershock epicentres for the two days after each of the major earthquakes; assuming that aftershock epicentres are above the regions faulted by the principal earthquakes, and that aftershock activity is highest immediately after a large shallow earthquake, it can be seen that faulting occurred in two distinctly different regions - one to the west of Buka (14 July) and the other in the offshore region adjacent to southeast New Britain and southern New Ireland (26 July). For each earthquake, the MM8 isoseismal roughly envelope the aftershock zone, and the intensities were apparently related to their distances from the earthquake fault surface, not their distances from the epicentre.

The two aftershock areas overlap to the southeast of southern New Ireland, and it was here that rupturing on 26 July started, presumably because of the effects of the 14 July earthquake series.

Other interesting features of the earthquake faulting are indicated by the hypocentral distribution of the aftershocks. Plots of hypocentres (mostly in the depth range 30-70 km) revealed a tendency for aftershock depths to increase with distance from the New Britain/Bougainville Trench, which coincides with the southern part of the epicentral area of aftershocks; i.e. contours of equal mean depths of aftershock hypocentres are arcs that subparallel the trends of the trench.

This effect may be seen in Figure 5, which shows ERL aftershock hypocentres in the western, northern, and eastern areas of the aftershock region projected onto vertical planes (A-B, A-C, and A-D in Fig. 4) normal to the tectonic trend. Each profile shows that focal depths (the eastern area is to the southeast of A-D, the western area is southwest of A-B and the northern area is bounded by ABCD.) increased with distance from Point A, i.e. away from the trench area.

Arrival times from Pomio (PNB), a temporary station situated above the westernmost part of the aftershock area, were used by ERL to improve the accuracy of focal depths in that area. The improvement is indicated by the thinness of the aftershock zone (about 20 km) nearest Pomio compared with that (40 km) indicated by the ERL determinations for which PNB data were not available. More accurate determination of the hypocentres may reveal a very thin aftershock zone.

The Pomio results also illustrate another feature, namely an increase with depth in the dip of the aftershock zone (Fig. 5, A-B plane). This effect is also noted in the zone of regional seismicity, which is shallow and dips shallowly beneath the northern Solomon Sea near the New Britain/Bougainville Trench but is very deep and dips steeply beneath New Britain the Bougainville (Denham, 1969), where it takes the form of a Benioff zone. For example, the envelope of 1959-1970 seismicity in the northern area of the aftershock zone when projected onto plane A-C (Fig. 5) shows the main seismic zone dipping more steeply to the north, whereas the group of earthquakes about 110 km deep on plane A-D illustrates the increase of dip with depth that takes place in the eastern aftershock area.

The pattern of aftershocks and regional seismicity shown on plane A-C (Fig. 5) also indicates that (a) the faulting associated with the principal earthquakes was in the upper part of the regional seismicity zone, and that (b) the faulting associated with the 26 July earthquake was probably an extension of faulting resulting from the 14 July earthquake (because aftershock hypocentres for the two intermingle).

The picture of faulting deduced from the aftershock pattern is that the two principal earthquakes each ruptured half of one arcuate fault zone that extends around the northern part of the Solomon Sea and is subparallel to the New Britain/Bougainville Trench. The faulting took place in the upper part of the regional seismicity zone; its dip averaged about 15-20° and increased with increasing depth of the aftershock zone.

Other evidence on the nature of faulting, namely the fault-plane solutions, will now be considered.

FAULT-PLANE SOLUTIONS

Plots of the first-motion data (Fig. 6) gave the fault-plane solution listed in Table 2. The solutions are fairly tight and agree well with those determined independently by Curtis (1973b). However, the solutions presented here are considered to be more accurate because all local network seismograms were used to obtain the results listed in Table 2.

Each solution indicates a major component of dip-slip faulting with the pressure axis plunging shallowly to the south-southwest; a minor component of sinistral strike-slip movement occurred during the earthquake of 26 July. The fault-plane solutions are ambiguous - the island arc may have either overthrust or underthrust the north Solomon Sea area - but overthrusting from the north is clearly indicated by the aftershock distribution and is consistent with the island-arc and trench structure, i.e. nodal plane 2 is considered to be the fault plane (at the point where rupturing commenced).

The directions of dip-slip fault movement (given by the azimuth of the pole of nodal plane 1) were 031° for the 14 July earthquake and 356° for the 26 July earthquake; each fault movement was normal to the tectonic trend at the epicentre of the principal earthquake. The dips determined for the fault surface were 40° (14 July) and 32° (26 July).

The dips indicated by the fault-plane solutions apply to the region where the earthquakes' first motions occurred, namely at the hypocentres (about 50 km deep), and agree well with the dip of the aftershock zone at this depth (Fig. 5). Had the epicentres of the principal earthquakes been closer to point A in Figure 5 the dips obtained from the first-motion study would have been less.

COMPARISON WITH THE ALASKAN EARTHQUAKE

A comparison of the combined features of the Solomon Sea earthquakes with those of the great Alaskan earthquake of 1964 is interesting because the three earthquakes are major events that occurred in similar tectonic environments.

For the Alaskan earthquake (see Fig. 7), the occurrence of topographic uplift and subsidence, the fault-plane results, and the distribution of aftershocks (Fig. 7) strongly indicated a shallow underthrusting of the continent (Plafker, 1965, 1972; Stauder & Bollinger, 1966); there was other less convincing evidence indicating a near-vertical dip-slip movement (Ben-Menahem, Rosenman & Israel, 1972).

Similar features of the earthquakes were:

(a) The aftershock epicentres at both places were concentrated in a broad, arcuate region (c.f. Figs. 4 and 7).

(b) The aftershock hypocentres for the Alaska series (see Page, 1968) and for both the Solomon Sea series occurred in the upper part of the regional seismicity zone.

(c) The directions of movement on the assumed fault plane for the two Solomon Sea earthquakes were roughly normal to the tectonic trends in the epicentral regions. Similarly Stauder & Bollinger (1966), using aftershock fault-plane solutions, showed that the direction of movement across the Alaskan fault plane changed systematically as the tectonic trend changed.

(d) The three earthquake series generated tsunamis.

With overthrusting taking place in the north Solomon Sea, uplift and subsidence should have occurred there. However, good evidence of ground movements in the area could not be expected because most of the fault zone was beneath the sea. Plafker's (1972) curves for deformations due to overthrust faulting show that minor subsidence could have occurred around the northeastern, northern, and northwestern areas of the Solomon Sea after-shock activities, and could have been visible in southern New Ireland and eastern New Britain. A systematic search for evidence of topographic changes has not been attempted, but is is known that major surface deformations on land did not occur.*

Tsunami data are sketchy, and insufficient to establish firm ideas on seafloor deformations. It suffices to note that (a) tsunamis did occur, and, hence, deformations must have taken place; (b) reliable reports from Rabaul, presumably outside the deformed zones, stated that after both earthquakes the sea first receded from the Rabaul shore; this indicates subsidence in the area of the north Solomon Sea where the fault plane was closest to Rabaul; and (c) the long period of the tsunamis, 25 minutes, indicates large source areas, and submarine landslides are unlikely to have caused such waves.

---

* The only known earthquake deformation on land in Papua New Guinea occurred on 2 February 1920 at Gasmata (6.2°S 150.3°E), where a reef was raised 0.6 metres (Pigot, 1923) as a result of an M7.7 earthquake.

MAGNITUDES

Because the rupture zones of both earthquake were at an average depth of about 50 km, 17 km deeper than normal (33km), the surface-wave magnitude would tend to be too small. Application of Bath's (1952) additive term (0.008h, where h is the depth departure from normal in km) for focal depth correction to the ERL surface-wave magnitude gives magnitudes of 8.0 for each earthquake. Also the body-wave magnitude determined by ERL, MB (ERL), would tend to be too small, because for large, relatively shallow earthquakes MB(ERL) values rarely exceed 6.0 (equivalent to 6.6 on the MS scale); the reason for this is that large earthquakes are multiple events and the first three cycles of the P wave, used to obtain MB(ERL), are due only to the start of the earthquake.

For the two earthquakes, the dimensions of the aftershock zone, and the maximum intensity, were employed to obtain magnitude values for comparison with the ERL determinations.

The areas over which aftershocks occurred within 48 hours of the main earthquakes are outlined in Figure 4; they were 1.6×10^4 km^2 and 2.0×10^4 km^2 for the 14 July and 26 July earthquakes respectively. Inserting these values in Utsu & Seki's (1954) relation between magnitude of a main shock and the aftershock area: $\log A = 1.02M - 4.0$ (where A is the aftershock area in km^2), we find magnitudes (MS) of 8.0 and 8.1. These are minimum values because the aftershock areas expanded slightly with lapse of time.

From a consideration of the lengths of the aftershock zones of the MS8.4 Alaskan earthquake (800 km) and the Solomon Sea earthquakes (average 280 km), and King & Knopoff's (1968, fig. 1) relation between fault length and magnitude, a magnitude of 8.0 for the Solomon Sea earthquakes seems likely.

Using Shebalin's (1956) relation between maximum intensity (I_o), magnitude (M), and depth (h) of an earthquake, $I_o = 1.5M - 3.5 \log h + 3$, a magnitude of 7.8 for both events is indicated. Again these values are minimum estimates because I_o is uncertain: the maximum intensity observed on land for both earthquakes was MM8+ (about 8.5), but the highest intensities were probably somewhere above the central part of the fault plane, i.e. offshore; hence, the true value of I_o could not be observed. A magnitude of 8.0 is obtained when a reasonable estimate of Io = MM9 is substituted in Shebalin's formula.

Considering all the relevant evidence a magnitude of 8.0 should be adopted for both earthquakes.

CONCLUSIONS

The following conclusions were reached:

(a) The two major north Solomon Sea tsunamigenic earthquakes of 14 July and 26 July 1971 were associated with overthrust faulting of two adjoining parts of one fault surface; this fault surface was arc-shaped in plan and in cross section.

(b) Faulting took place in the upper part of the regional seismicity zone at depths ranging from about 30-70 km.

(c) The dip of the fault surface averaged 15° - 20°, but increased as the fault surface deepened with distance north of the New Britain/Bougainville Trench.

(d) Fault-plane solutions for the principal earthquakes show that movements at the fault surface tended to be normal to the tectonic trends at the epicentres; the dips agree with those suggested by the aftershock pattern.

(e) Features of the combined aftershock pattern and the fault-plane solutions resembled those of the major 1964 Alaskan earthquake.

(f) The mean isoseismal radii for both principal earthquakes were about the same for a given intensity. The maximum intensities were greater than MM8. Isoseismals for the higher intensities were elliptical with the long axis trending north-northwest for the 14 July earthquake and east-northeast for the 26 July earthquake. Intensity of shaking was directly related to distance from the relevant earthquake fault zone.

(g) The surface-wave magnitude of both earthquakes was about 8.0.

(h) Ground deformation due to faulting was not observed, but the generation of tsunamis suggests that it did take place beneath the north Solomon Sea.

ACKNOWLEDGEMENTS

The services of the office of District Administration and the Director, Civil Defence and Emergency Services, Port Moresby, in supplying information on the earthquakes' effects are gratefully acknowledged. The paper is published with permission of the Director, Bureau of Mineral Resources, Canberra.

REFERENCES

BATH, M., 1952: Earthquake magnitude determination from the vertical component of surface waves. Trans. Amer. geophys. Un., 33, 81-90.

BEN-MENAHEM, A., ROSENMAN, M., & ISRAEL, M., 1972: Source mechanism of the Alaskan earthquake of 1964 from amplitudes of free oscillations and surface waves. Phys. Earth. Planet. Interiors, 5, 1-29.

BROOKS, J.A., 1965: Earthquake activity and seismic risk in Papua New Guinea. Bur. Miner. Resour. Aust. Rep. 74.

CURTIS, J.W., 1973a: Spatial seismicity of Papua New Guinea. J. geol. Soc. Aust., 20, 1-19.

CURTIS, J.W., 1973b: Plate tectonics and the Papua-New Guinea - Solomon Islands region. J. geol. Soc. Aust., 20, 21-36.

DENHAM, D., 1969: Distribution of earthquakes in the New Guinea - Solomon Islands region. J. geophys. Res., 74, 4290-9.

DIETERICH, J.H., 1972: Time-dependent friction as a possible mechanism for aftershocks. J. geophys. Res., 77, 20, 3771-81.

EVERINGHAM, I.B., in press: The major Papua New Guinea earthquake near Madang (1970) and beneath the north Solomon Sea (1971). Proc. 5th World Conf. Earthq. Eng., Rome, June 1973.

GUTENBERG, B., & RICHTER, C.B., 1954: SEISMICITY OF THE EARTH (2nd Ed.) Princeton. Univ. Press, 310 pp.

JOHNSON, T., & MOLNAR, P., 1972: Focal mechanism and plate tectonics of the southwest Pacific. J. geophys. Res., 77 (26), 5000-32.

KING, C., & KNOPOFF, L., 1968: Stress drop in earthquakes. Bull. seism. Soc. Amer., 58, 249-57.

LUYENDYK, B.P., MACDONALD, K.C., & BRYAN, W.B., 1973: Rifting history of the Woodlark Basin in the southwest Pacific. Bull. geol. Soc. Amer., 84, 1125-34.

PAGE, R., 1968: Aftershocks and microaftershocks of the great Alaska earthquake of 1964. Bull. seism. Soc. Amer. 58, 1131-68.

PIGOT, E.F., 1923: Brief notes regarding earthquakes in the New Guinea region. New Guinea Ann. Rep. for 1921-22, 104 (Appendix E).

PLAFKER, G., 1965: Tectonic deformation associated with the 1964 Alaska earthquake. Science, 148, 1675-87.

PLAFKER, G., 1972: Alaskan earthquake of 1964 and Chilean earthquake of 1960: implications for arc tectonics. J. geophys. Res., 77, 901-25.

SHEBALIN, N.V., 1956: The relation between intensity and magnitude of an earthquake with respect to focal depth. Akad. Nauk. SSSR Soviet Po Sysmologii Bull., 6, 122-6.

STAUDER, W., & BOLLINGER, G.A., 1966: The focal mechanism of the Alaska earthquake March 28, 1964 and of its aftershock sequence. J. geophys. Res., 71, 5283-96.

UTSU, T., & SEKI, A., 1954: A relation between the area of aftershock regions and the energy of main shock. Zisin., Ser. 2, 7, 238.

TABLE 1

MEAN ISOSEISMAL RADII

Date	Mean Radius			
1971	MM8	MM7	MM6	MM5
14 July	(85)	160	250	(320)
26 July	130	190	270	420

Note: ( ) less accurate values

All values are fairly inaccurate as the isoseismals were interpreted over large areas of sea.

TABLE 2

FAULT-PLANE SOLUTIONS

	Pole of Nodal Plane 1		Pole of Nodal Plane 2		T Axis		P Axis	
Date	Az°	P1°	Az°	P1°	Az°	P1°	Az°	P1°
14 July	031	040	200	050	070	082	206	005
26 July	356	020	232	058	324	055	195	024

To accompany Record No. 1974/55

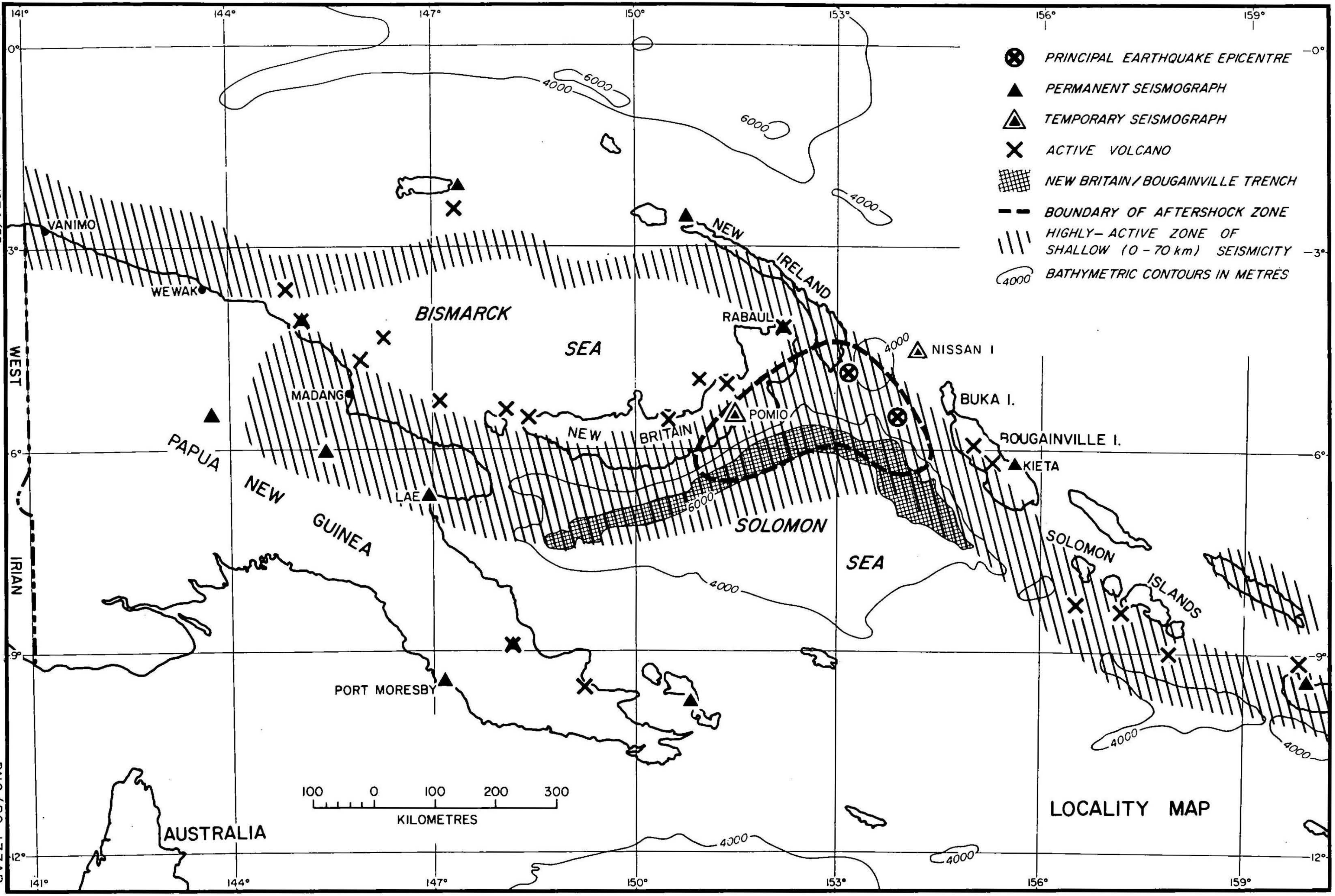

Fig. I

PNG/B9-177AR

Fig. 2

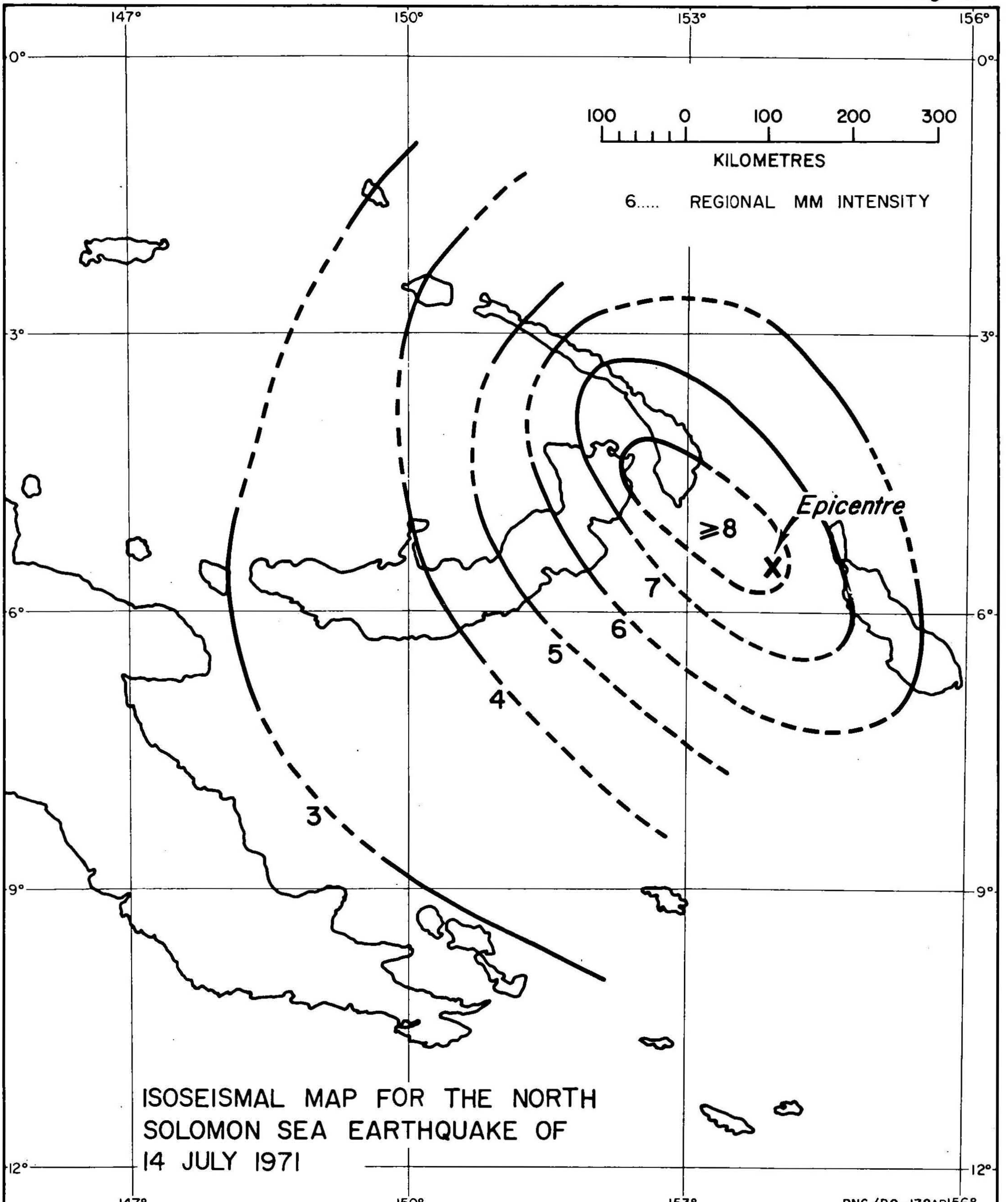

To accompany Record No. 1974/55

Fig. 3

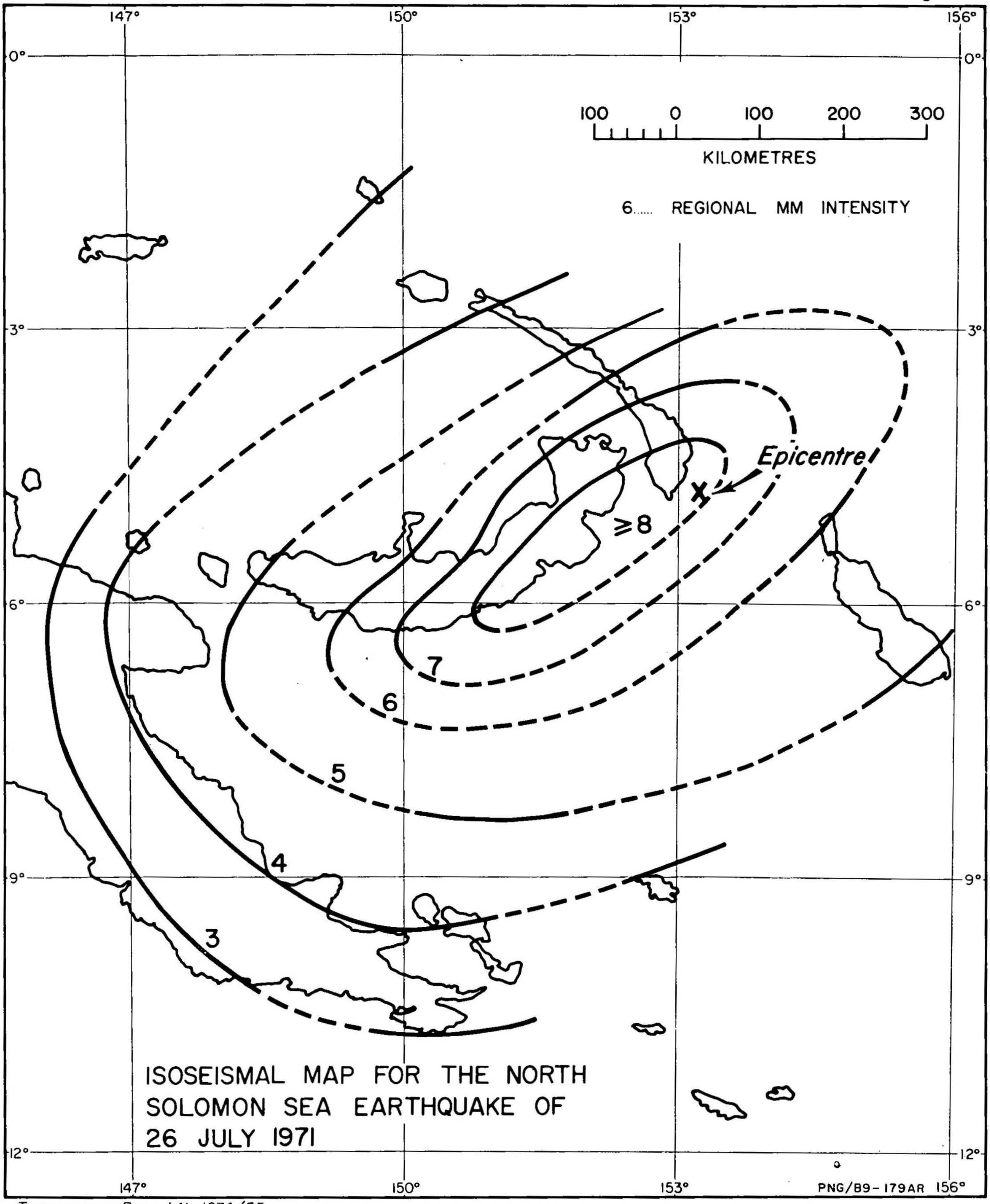

To accompany Record No. 1974/55

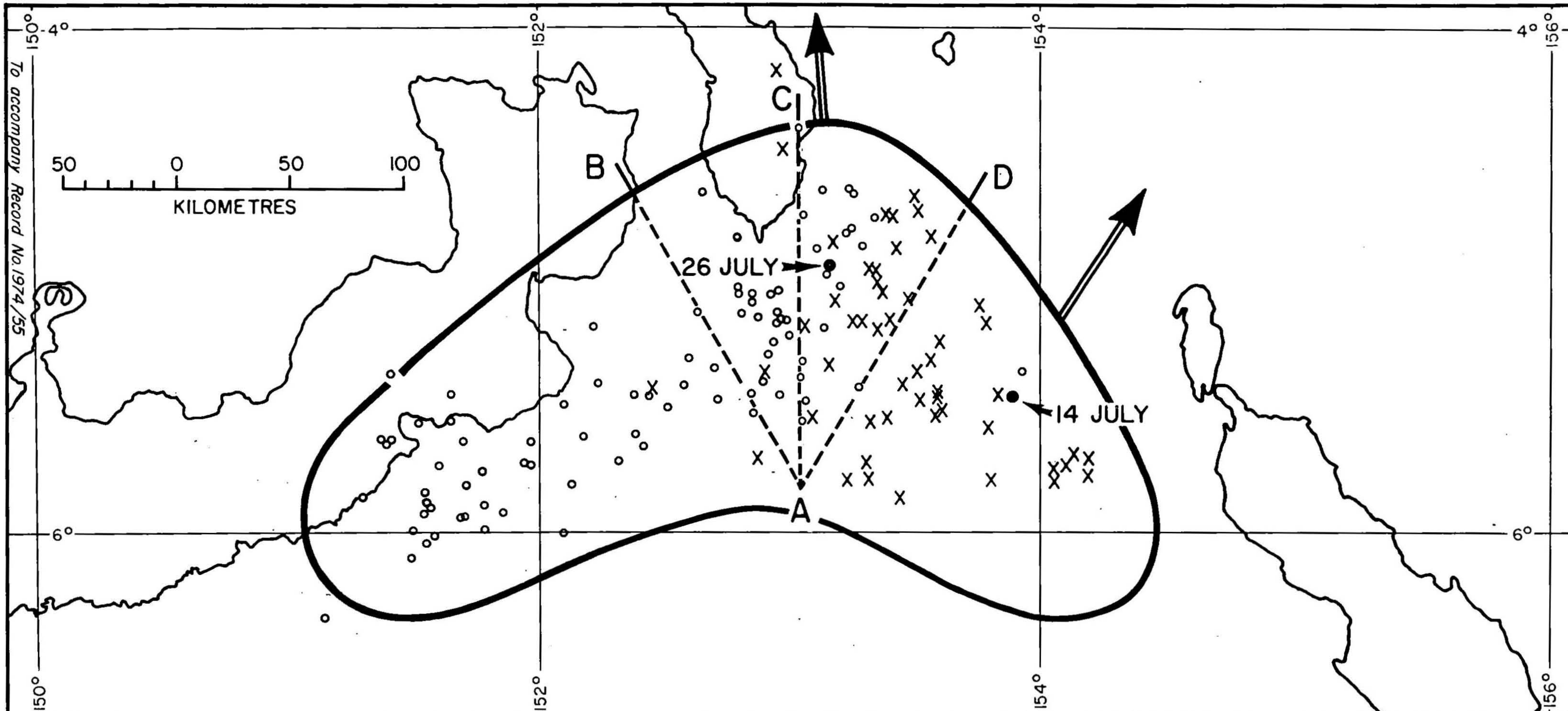

• Principal earthquake epicentre

x Aftershock epicentres for period of two days after 14 July principal earthquake

o Aftershock epicentres for period of two days after 26 July principal earthquake

⟸ Direction of fault slip

Boundary of aftershock region, 14 July to 31 August

A — — B Vertical plane used for fig. 5 profiles

AFTERSHOCK AREAS

Fig. 4

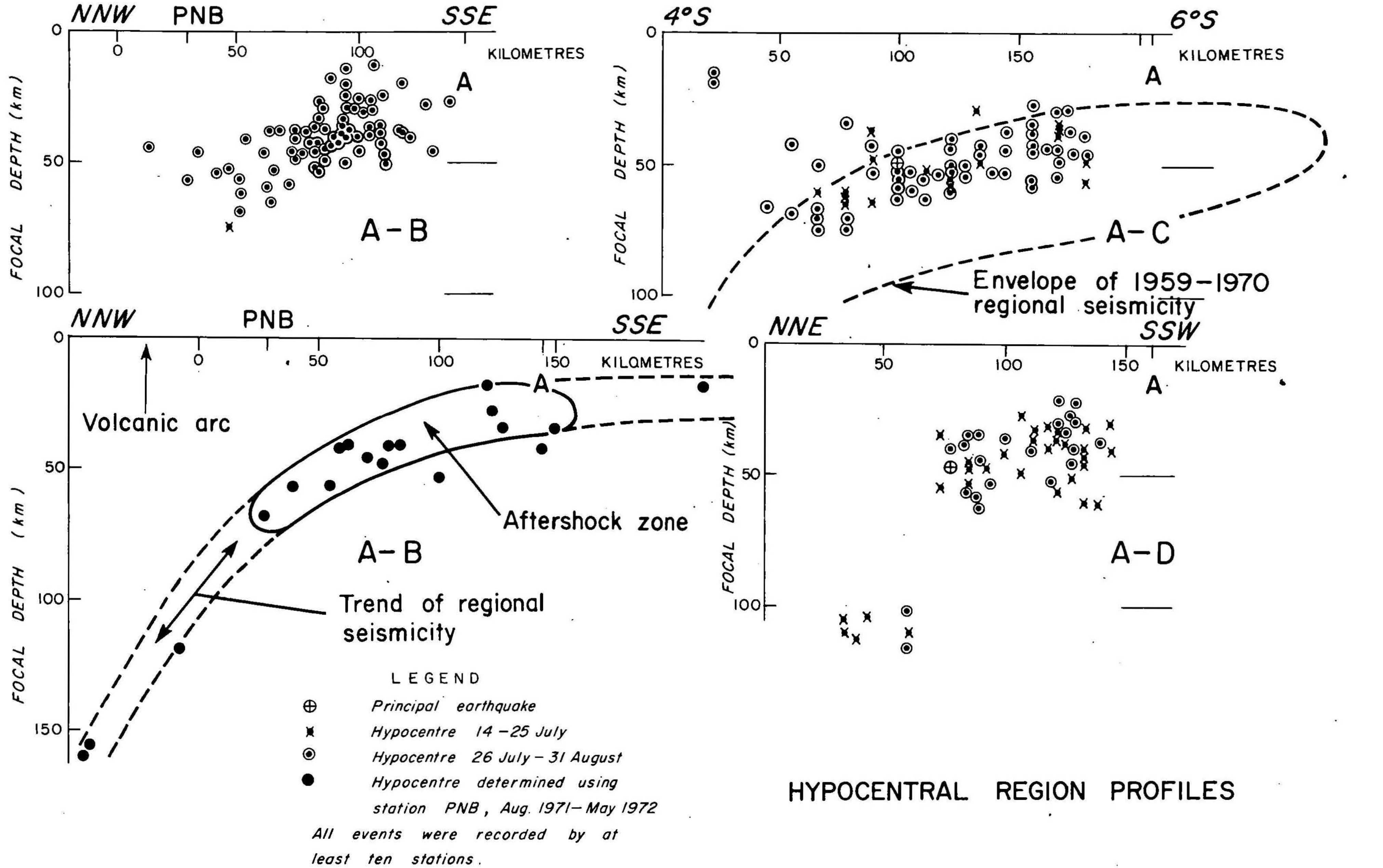

HYPOCENTRAL REGION PROFILES

To accompany Record No. 1974/55

PNG/B9-182A

Fig. 5

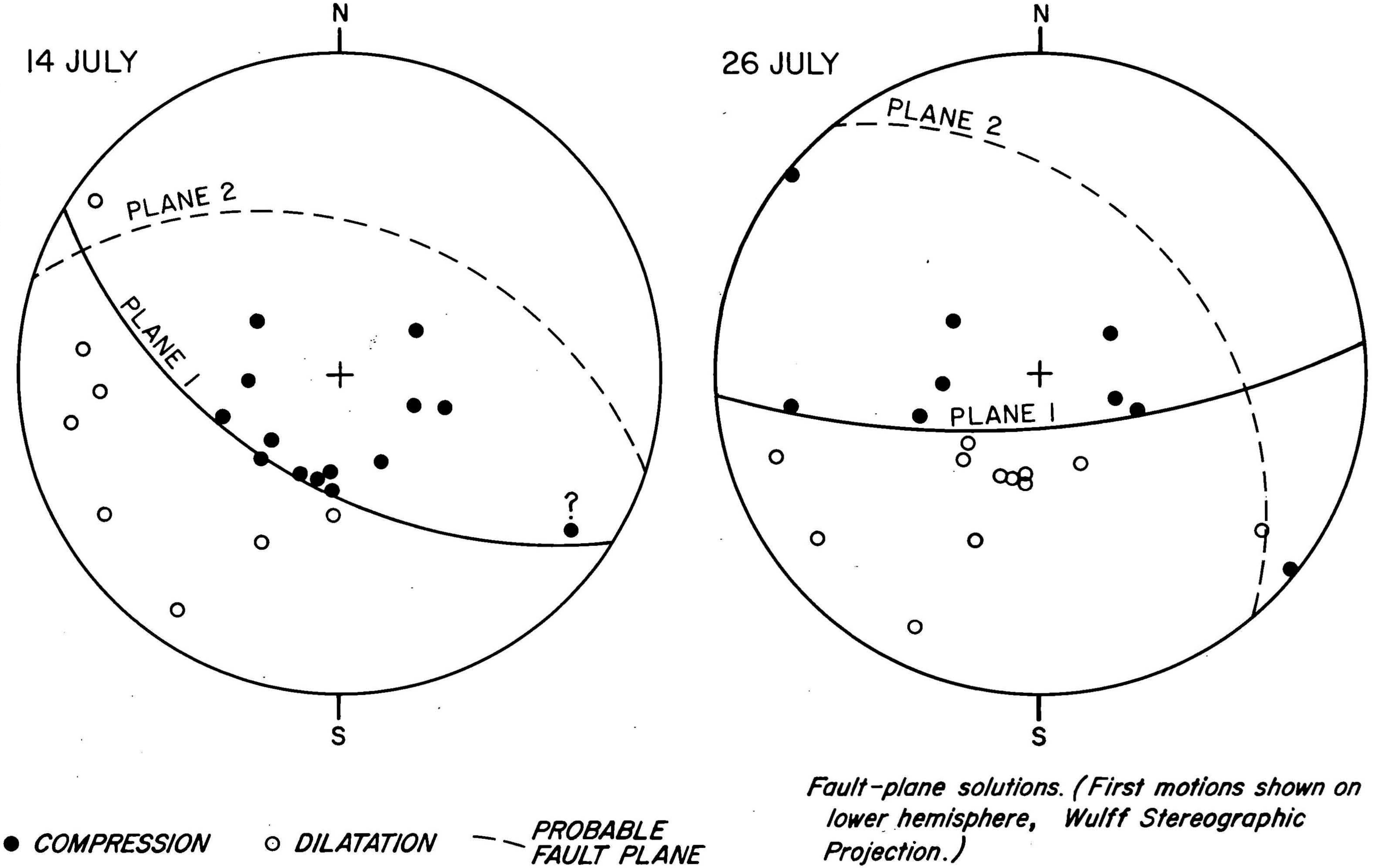

Fault-plane solutions. (First motions shown on lower hemisphere, Wulff Stereographic Projection.)

To accompany Record No. 1974/55

PNG/B9-181A

Fig. 6

Fig. 7

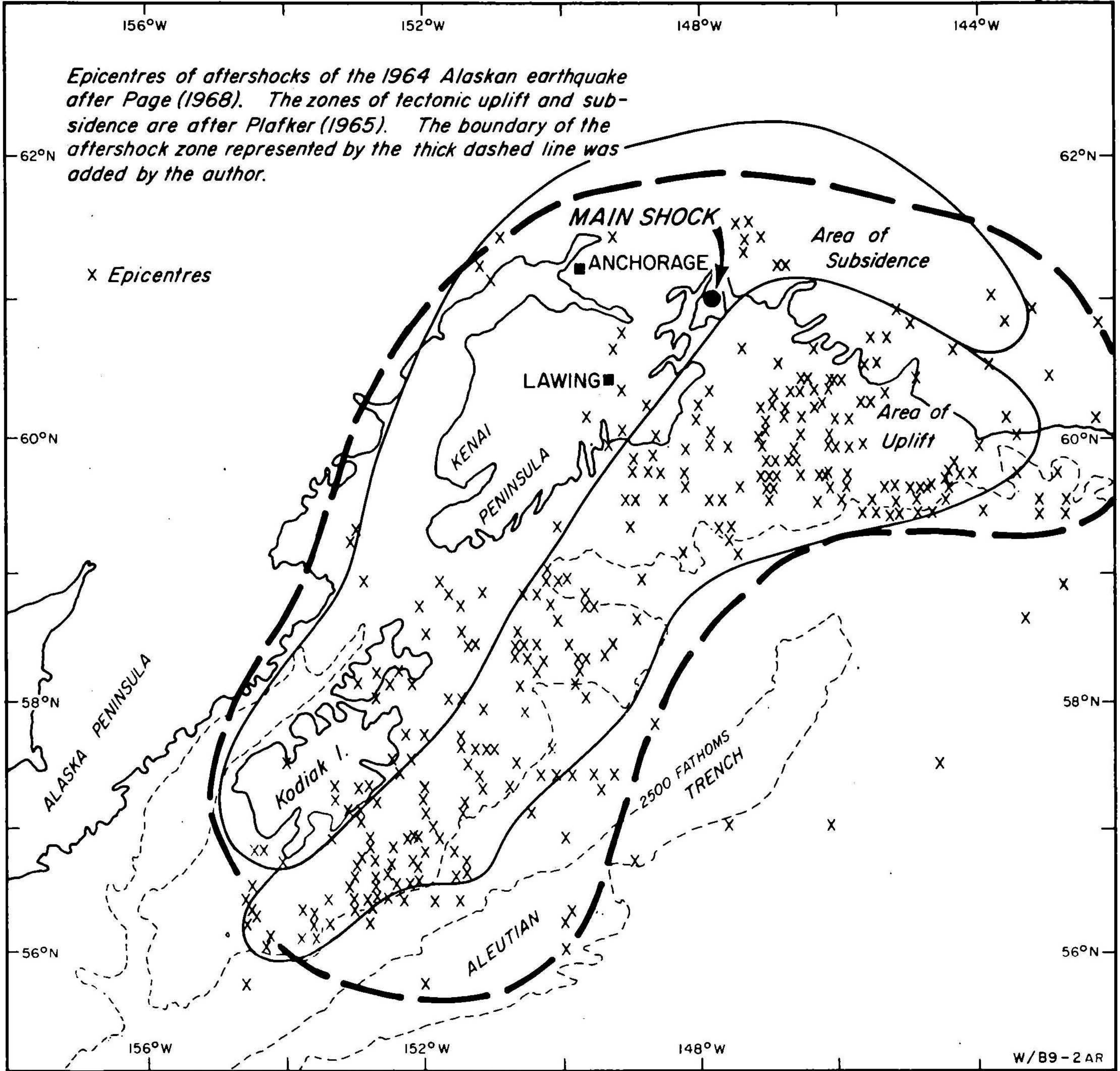

To accompany Record No.1974/55